Biochimica et Biophysica Acta, 401 (1975) 416–428

BBA 77043

ACCELERATIVE EXCHANGE DIFFUSION KINETICS OF GLUCOSE BETWEEN BLOOD AND BRAIN AND ITS RELATION TO TRANSPORT DURING ANOXIA

A. LORRIS BETZ, DAVID D. GILBOE and LESTER R. DREWES

Departments of Neurosurgery, Physiology and Biochemistry, University of Wisconsin, Madison, Wisc. 53706 (U.S.A.)

(Received January 24th, 1975)

SUMMARY

An earlier study showed that unidirectional glucose transport from blood to brain decreases during perfusion with anoxic blood (Betz, A. L., Gilboe, D. D. and Drewes, L. R. (1974) Brain Res. 67, 307–316). Brain glucose levels also decrease during anoxia. Therefore, the present study was designed to investigate whether the decreased transport might be the result of decreased accelerative exchange diffusion when brain glucose levels are low.

The rate of unidirectional transport into brain (v) of D-[6-^{3}H]glucose was studied in 22 isolated, perfused dog brains by means of an indicator dilution technique using ^{22}Na as the intravascular reference. The kinetics of transport were determined over a range of blood glucose concentrations (S_1) at each of five different brain glucose levels (S_2). The existence of accelerative exchange diffusion for glucose was indicated by a decrease in the intercept (increase of apparent V) of a double reciprocal plot ($1/v$ versus $1/S_1$) as S_2 increased. This phenomenon is consistent with a model for facilitated diffusion in which the mobility of the loaded carrier is greater than that of the unloaded carrier. Although the data predict a decrease in glucose transport during anoxia, the predicted decrease (5 %) is less than the observed decrease (35 %). It is concluded that the simple mobile-carrier model for facilitated diffusion cannot, by itself, describe all properties of blood-brain glucose transport.

INTRODUCTION

It is generally accepted that the movement of sugars across cell membranes does not occur by simple diffusion, but rather is mediated through a specific interaction with some membrane component. Available evidence indicates that there are at least three basic sugar transport mechanisms. In some bacteria, monosaccharide transport appears to be directly coupled to an energy source and thus is capable of promoting accumulation against a concentration gradient [1, 2]. Such systems are known as primary active transport. Secondary active (coupled) transport can also promote sugar accumulation, however, instead of requiring a direct source of energy,

transport is coupled to ion gradients. Na^+-linked sugar transport occurs in the intestine and kidney [2, 3], while it has been proposed that H^+-coupled transport is present in bacteria [1, 2]. Non-accumulating carrier-mediated monosaccharide transport that is dependent on neither energy nor ion gradients has been studied in erythrocytes, muscle, placenta and other mammalian tissues [2]. This type of transport is called facilitated diffusion. Kotyk [4] and Wyssbrod et al. [5] have recently reviewed kinetic models for all three classes of transport.

On the basis of studies showing that whole brain glucose levels do not exceed blood glucose concentrations, Buschiazzo et al. [6] have proposed that carrier-mediated transport of sugars across the blood-brain barrier occurs by a facilitated diffusion mechanism. There is little additional evidence to support this hypothesis. We have recently demonstrated that unidirectional glucose transport from blood to brain is significantly decreased after 10 min of anoxic perfusion [7]. These data appear to indicate that an active transport process may be involved. An alternative hypothesis, however, is that the decreased brain glucose levels that occur during anoxia cause a reduction in accelerative exchange diffusion of glucose from blood to brain. This phenomenon, which has been observed using several different solutes in various tissues [8–11], is generally thought to occur in carrier-mediated systems when the mobility of the loaded carrier is greater than that of the unloaded carrier.

The present study was designed to determine the effect of the brain glucose concentration on the rate of unidirectional glucose transport into the isolated, perfused dog brain. These data can then be compared to changes in the rate of unidirectional glucose transport that occur during anoxia.

METHODS

Brain isolation and perfusion

Brains were isolated without interruption of circulation from 22 adult mongrel dogs (15–20 kg) that were anesthetized with halothane. The procedure that was used [12] involves removal of all extracranial soft tissue and leaves the brain intact within the cranium. The spinal cord is transected at the level of the second cervical vertebra. Arterial blood is supplied through the internal carotid arteries and the anastomotic branch of the internal maxillary arteries. Venous blood is collected through a threaded Luer connector cemented over a small hole drilled into the bone covering the confluence of sinuses.

The perfusate consisted of compatible donor blood that had been diluted with dextran to a hematocrit of about 24–28 % and conditioned [13]. Blood with low glucose concentrations was obtained from donor dogs that received from 10 to 20 I.U. of regular insulin at the time blood conditioning was begun. We have previously demonstrated that insulin has no effect on unidirectional glucose transport into brain [14]. The viability of the preparation was assessed at frequent intervals from electroencephalographic recordings and oxygen consumption determinations. At the termination of each experiment, the brain was removed and weighed.

The perfusion apparatus consisted of two separate pump-oxygenator systems interconnected through a valve that permitted perfusion from only one oxygenator at a time [13]. One system was used to equilibrate the brain at a given, fixed glucose level and to maintain the preparation between determinations of glucose transport. The

second system contained identical blood except that the glucose concentration was varied in increments from values lower to values higher than those of the maintenance system. This configuration permitted us to determine the rate of glucose transport immediately following a sudden change in the glucose concentration of blood perfusing the brain. The indicator dilution technique was used to measure unidirectional glucose transport over a range of blood glucose concentrations on those brains that were equilibrated at various fixed glucose levels. Fishman [15] has shown that about 75 min are required for cerebrospinal fluid glucose levels to plateau following a sudden increase in the blood glucose concentration. Therefore, to permit equilibration of the brain with high maintenance blood glucose levels, indicator dilution experiments were not performed during the first 60 min after brain isolation.

Indicator dilution injections

Although the indicator dilution technique has been described in detail elsewhere [14], the procedure will be briefly summarized here. The 50 μl-injectate contained 2 μCi of ^{22}Na, the intravascular marker, and 10 μCi of D-[6-^{3}H]glucose, the test molecule. 15 s before each indicator dilution injection, the valve was switched to start brain perfusion at the experimental glucose concentration. A 50-μl syringe was used to inject the isotope mixture directly into the common carotid artery near the internal carotid bifurcation. Sampling started 3 s after the injection. 30 consecutive venous blood samples were collected at 1-s intervals and then arterial and venous samples were taken for glucose analysis. The blood flow rate was determined by measuring the volume of a 1 min collection of venous blood. Then the valve was switched to re-equilibrate the brain at the maintenance perfusate glucose level.

Blood samples were digested and decolorized for simultaneous liquid scintillation counting of ^{22}Na and ^{3}H by the H_2O_2–$HClO_4$ method described in a prior study [14]. Plasma arterial and venous glucose concentrations were determined in triplicate by a glucose oxidase method using a Beckman glucose analyzer.

Tissue glucose determination

At the end of eight experiments, the maintenance glucose level was adjusted to an arbitrary value and, after 20 min of equilibration, cerebral cortex samples were collected by freezing in situ [16]. Tissue glucose was extracted into 6 % $HClO_4$ and assayed enzymatically [17].

Anoxic experiments

Changes in the rate of transport that occurred during anoxic perfusion were observed in four isolated brain preparations. The blood in the maintenance and experimental systems was identical except that the pO_2 in the experimental oxygenator was reduced to less than 10 mmHg by equilibration with N_2 and CO_2 instead of air and CO_2. Therefore, anoxia could be initiated simply by switching to the experimental oxygenator. Blood glucose levels were maintained between 5.0 and 6.5 mM in both systems. Indicator dilution injections were made before, and at 2, 5, 10, 15, 20, 25, 30, 35, 40, 45, 50, 55 and 60 min after, the onset of anoxia.

Calculations

The data treatment that was used [14] permits calculation of the maximal glu-

cose extraction from the blood, E, for each indicator dilution injection that was made. Since the rate of unidirectional glucose uptake depends upon the plasma flow rate as well as the capillary glucose concentration [14], all indicator dilution injections were made at plasma flow rates between 0.45 and 0.55 ml/g of brain per min. The rate of glucose uptake, u, can be calculated from the equation $u = ES_aF_p/W$ where S_a is the arterial plasma glucose concentration, F_p is the plasma flow rate and W is the brain weight. However, on the basis of experiments with [^{3}H]fructose, we have estimated that the rate of simple diffusion of glucose into the brain is 3.6 % [14]. Therefore, the rate of unidirectional glucose transport into the brain, v, was calculated by incorporating this diffusion correction into the glucose uptake equation, i.e. $v = (E-0.036)S_aF_p/W$.

Data for glucose transport at each of the five different maintenance glucose levels were fitted to the Michaelis-Menten equation which describes carrier-mediated transport when brain glucose is constant (see Appendix).

$$v = \frac{V_{app}S_1}{K_{app}+S_1}$$

S_1, the average of the arterial and venous glucose concentrations, is used as an approximation of the average glucose concentration in the capillary and V_{app} and K_{app} are the apparent kinetic constants for transport. A computer program that utilizes an iterative, least-squares method to fit this equation was used to calculate K_{app}, V_{app} and their respective standard errors [18]. Weighting factors were used to increase the accuracy of the fit as described previously [14].

RESULTS

Indicator dilution injections were made over a range of blood glucose levels (S_1) on 18 brains equilibrated with five different maintenance perfusate glucose con-

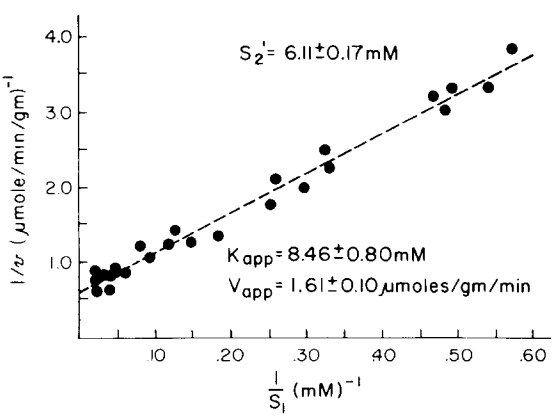

Fig. 1. Representative data showing the kinetics of unidirectional transport into brain at a constant brain glucose concentration. Five brains were equilibrated with a fixed blood glucose concentration (S'_2) during maintenance perfusion and unidirectional transport (v) was determined about 30 s after initiating perfusion at the experimental glucose concentration (S_1). Data are shown as a double reciprocal plot derived from a direct fit to the Michaelis-Menten equation. Values for K_{app} and V_{app} are given ± 1 S.E.

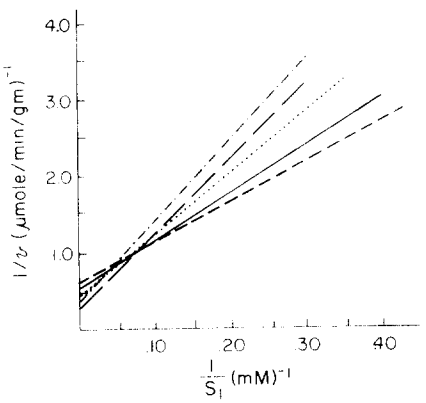

Fig. 2. Kinetics of unidirectional tranport into brain at various glucose concentrations. Brains were equilibrated at five different levels of blood glucose and data were obtained by the method summarized in the legend to Fig. 1. Each represents the best fit to data obtained at a single value of S'_2. The values for S'_2 and the apparent kinetic constants with their corresponding S.E. were: - - -, 5 brains, S'_2 6.11 ± 0.17 mM, K_{app} 8.46 ± 0.80 mM, V_{app} 1.61 ± 0.10 μmol/g per min, N 25; ——, 3 brains, S'_2 16.8 ± 0.3 mM, K_{app} 11.2 ± 1.5 mM, V_{app} 1.84 ± 0.16 μmol/g per min, N 17; · · ·, 2 brains, S'_2 26.3 ± 0.2 mM, K_{app} 17.7 ± 2.3 mM, V_{app} 2.21 ± 0.21 μmol/g per min, N 17; - · - · -, 4 brains, S'_2 43.9 ± 0.6 mM, K_{app} 28.2 ± 6.3 mM, V_{app} 2.68 ± 0.44 μmol/g per min, N 23; , 4 brains, S'_2 56.0 ± 1.2 mM, K_{app} 37.7 ± 13.5 mM, V_{app} 3.83 ± 1.10 μmol/g per min, N 19.

centrations (S'_2). Fig. 1 is a double reciprocal plot of the data obtained when S'_2 6.11 mM. Data obtained at other S'_2 levels were similar and are summarized in Fig. 2. From these plots it is obvious that, as brain glucose increases, the slope increases while the intercept decreases. This relationship is better defined in Fig. 3, where the slopes and intercepts are plotted as a function of the glucose concentration with which the brain is equilibrated (S'_2). The hyperbolic activation seen in the intercept replot is

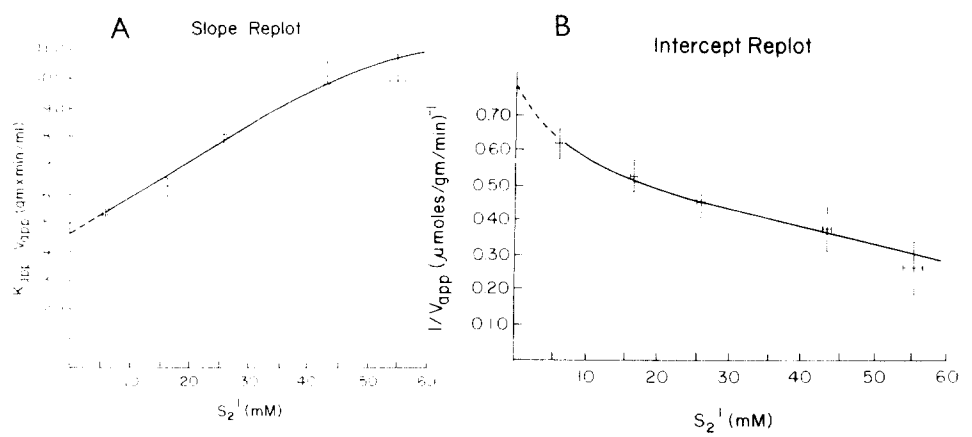

Fig. 3. Slope and intercept replots. The slopes (A) or intercepts (B) of the data in Fig. 2 are plotted as a function of the blood glucose concentration with which the brain was equilibrated (S'_2). Data are shown as averages ± 1 S.E.

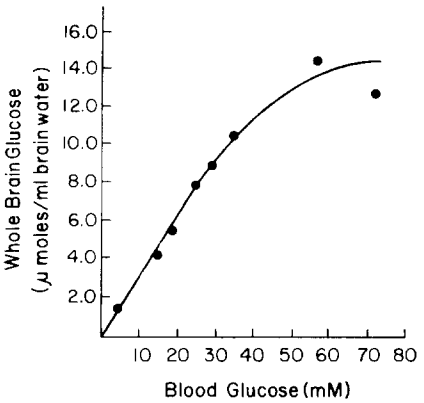

Fig. 4. Whole brain glucose concentration as a function of blood glucose concentration. Tissue glucose levels were corrected for a trapped blood glucose volume of 3 % and brain water content of 0.75 ml/g of brain [16]. Each value represents the average for duplicate samples from a single brain.

consistent with a stimulation in unidirectional influx due to accelerative exchange diffusion.

Fig. 4 shows the relationship between whole brain and perfusate glucose concentrations. The whole brain glucose level is approximately a linear function of blood glucose between 5 and 40 mM. However, brain water is probably decreased due to osmotic dehydration when blood glucose levels are greatly elevated. Therefore, corresponding brain glucose levels are lower than expected. Buschiazzo et al. [6], reported a sigmoidal relationship between blood and brain glucose in the rat, but this effect was not apparent until the blood glucose dropped well below the range of S'_2 values used in our study.

The results of experiments performed during perfusion with anoxic blood are shown in Fig. 5. These data are comparable to the pattern observed in a previous study of the effect of anoxia on unidirectional glucose transport [7].

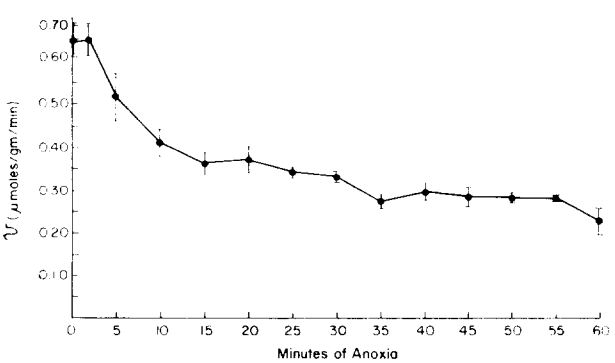

Fig. 5. Glucose transport during anoxia. The unidirectional transport of glucose was determined before, and at various times after, the initiation of perfusion with anoxic blood. The average capillary glucose concentration (S_1) during this time period was 5.23 mM ± 0.05 S.E. Transport rates are shown as averages ± 1 S.E. ($N = 4$).

DISCUSSION

This study clearly demonstrates that the apparent kinetic constants for unidirectional transport of glucose from blood to brain are a function of the brain glucose concentration. Regardless of the mechanism responsible for this effect, one must conclude that accurate evaluation of potential transport modifiers requires careful control of brain glucose levels. We have previously shown an effect of blood flow rate on cerebral glucose transport [14]. At present, only the isolated brain permits one to determine unidirectional transport from blood to brain while controlling both the cerebral blood flow rate and the brain and blood substrate concentrations. Apparent kinetic constants for transport, however, are valid only for the specific perfusion conditions used.

Although the exact location of transport systems that are observed with the indicator dilution technique is unknown, they are generally thought to be located at the site of the so-called blood-brain barrier [19–21]. Histochemical studies suggest that it is the capillary endothelium that restricts brain permeability to polar solutes [22]. Therefore, the glucose concentration within the capillary endothelial cell is probably responsible for the changes in kinetic constants that we observe (S_2 in Fig. 6). A similar transport step would be required to move glucose out of the endothelial cell and into the brain extracellular space. Previous studies have shown that there are at least two metabolically distinct glucose compartments in the brain [7, 23]. Cremer and Heath [23] observed a very rapid equilibration of glucose between one of these compartments and blood. Therefore, it appears likely that the steady-state glucose concentration within the capillary endothelial cell is a linear function of blood glucose, which is the same relation we observe between blood glucose and whole brain glucose.

As shown in the Appendix, hyperbolic slope and intercept replots are predicted for the mobile-carrier model of facilitated diffusion provided that (a) carrier translocation is not rate limiting and/or (b) the rates of translocation for loaded and unloaded carrier are unequal. Although one cannot be certain of the hyperbolic nature of the plots in Fig. 3, these data illustrate the phenomenon of accelerative exchange diffusion. Therefore, transport from blood to brain cannot be described by a simple symmetric carrier system.

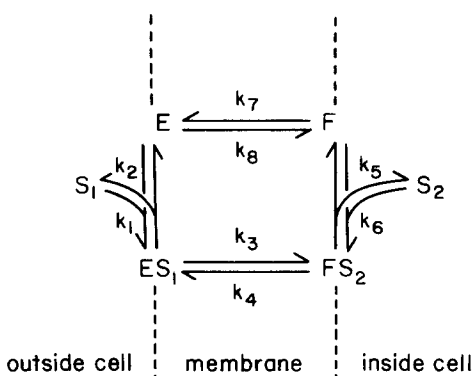

Fig. 6. General model for facilitated diffusion.

Glucose transport in the rabbit erythrocyte conforms to the simple symmetric model [24]: however, a more general model was required to explain glucose transport in the human erythrocyte [11, 25]. Although this model provided a far better fit to the data than the symmetrical model, several discrepancies remained. Recently, Regen and Tarpley [26] have obtained an improved fit to the general model by incorporating diffusion barriers between the carrier and the bulk aqueous phases both inside and outside the cell (unstirred layers). Other investigators have abandoned the mobile-carrier model altogether [27–29]. The system is apparently more complex than can be explained by any simple mobile-carrier model alone and quite clearly more data are required before an adequate description of the mechanism can be made.

Next one must ask: do our data predict the decrease in unidirectional glucose transport that is observed during anoxia? The predicted decrease would be the ratio of the velocity at $S_2 = 0$ to the velocity at $S'_2 = 6.1$ mM, $v_0/v_{6.1}$. $v_{6.1}$ was derived by using $S_1 = 5.23$ mM and K_{app} and V_{app} when $S'_2 = 6.1$ mM (Fig. 1). If S'_2 (Fig. 3) is extrapolated to $S'_2 = 0$ (whole brain glucose levels are near zero after 30 min of anoxia [30]), v_0 is determined. Thus the predicted ratio: $v_0/v_{6.1}$ is 0.95. When the rate of unidirectional transport after 30 min of anoxia is compared to the pre-anoxic control value (Fig. 5), the ratio $v_{30\,min}/v_{cont}$ is 0.65. It is unlikely that such a large difference could be accounted for by errors in extrapolation of the slope and intercept replots to zero. Thus, decreased exchange diffusion does not by itself explain the reduced rate of blood-brain glucose transport during anoxia. Batt and Schacter [31] have reported analogous results for glucose transport in the human erythrocyte. Using the general model of Regen and Morgan [24] they found that K_1 and V_1 values were greatly reduced for transport into cells containing no glucose when compared to transport into cells equilibrated with external glucose. The simple mobile-carrier model requires that these constants be independent of glucose concentration. Similar results were obtained with 3-*O*-methylglucose, suggesting that the metabolism of D-glucose was not essential for sugar transport. Batt and Schacter propose that this system exists in two states and that "transition from one state to the other is dependent on the presence of intracellular hexose" [31].

Alternative explanations for our data are that (a) glucose is actively transported across the blood-brain barrier by some mechanism that permits significant uptake when cerebral energy reserves are extremely low, (b) an inhibitor of glucose transport is produced during anoxia, or (c) there is a substantial redistribution of cerebral blood flow during anoxia. The first possibility could be the result of a transport system that involves both active transport and facilitated diffusion. Models for such systems have been developed by Rosenberg and Wilbrandt [32] and Silverman and Goresky [33]. We have no evidence to support or refute the second hypothesis. The third possibility appears to be unlikely in light of preliminary studies of regional blood flow performed during anoxia using the microsphere technique (Drewes, L. R. and Levin, A. B., unpublished results). Furthermore, unidirectional leucine transport is unchanged after 10 min of anoxia [19].

In addition, studies of the effect of transport inhibitors such as glucose analogues, phlorizin and phloretin (Betz, A. L., unpublished results) on transport from blood to brain yield results that are similar to those obtained with the human erythrocyte. We, therefore, believe that glucose transport across the blood-brain barrier is analogous to glucose transport in the human erythrocyte and that

neither system can be described by the simple mobile-carrier model of facilitated diffusion.

APPENDIX

Derivation of kinetic equations for the simple mobile-carrier model of facilitated diffusion

A. Assumptions. A schematic representation of a commonly used model for facilitated diffusion is shown in Fig. 6. Since net transport cannot occur against a concentration gradient, K_{eq} 1. The following kinetic equations are derived with only two simplifying assumptions, namely (a) each carrier molecule binds one substrate molecule and (b) the total amount of carrier is constant.

B. Net transport. The rate of net transport of substrate from one side of the membrane to the other is given by Eqn 1,

$$r_{net} \quad k_1 S_1[E] \quad k_2[ES_1] \tag{1}$$

where S_1 is the concentration of substrate on one side of the membrane. The concentrations of E and ES_1 can be derived using the method of King and Altman [34].

$$[E] \quad (k_7(k_3k_5 + k_2k_5 + k_2k_4) + k_2k_4k_6S_2)E_t/\text{Denominator}$$

$$[ES_1] \quad (k_1k_7(k_4 + k_5)S_1 + k_4k_6k_8S_2 + k_1k_4k_6S_1S_2)E_t/\text{Denominator}$$

$$\text{Denominator} \quad (k_7 + k_8)(k_3k_5 + k_2k_5 + k_2k_4) + k_1(k_3k_7 + k_4k_7 + k_5k_7 + k_3k_5)S_1 + k_6(k_2k_8 + k_3k_8 + k_4k_8 + k_2k_4)S_2 + k_1k_6(k_3 + k_4)S_1S_2$$

Substitution into Eqn 1 yields:

$$r_{net} \quad (k_1k_3k_5k_7S_1 \quad k_2k_4k_6k_8S_2)E_t/\text{Denominator} \tag{2}$$

where E_t is the total carrier present in the membrane, i.e.

$$E_t \quad [E] + [ES_1] + [F] + [FS_2]$$

Using the conventions of Cleland [35], the following relationships can be defined:

$$V_1 = \frac{k_1k_3k_5k_7E_t}{k_1(k_3k_7 + k_4k_7 + k_5k_7 + k_3k_5)}$$

$$V_2 = \frac{k_2k_4k_6k_8E_t}{k_6(k_2k_8 + k_3k_8 + k_4k_8 + k_2k_4)}$$

$$K_1 = \frac{(k_7 + k_8)(k_3k_5 + k_2k_5 + k_2k_4)}{k_1(k_3k_7 + k_4k_7 + k_5k_7 + k_3k_5)}$$

$$K_2 = \frac{(k_7 + k_8)(k_3k_5 + k_2k_5 + k_2k_4)}{k_6(k_2k_8 + k_3k_8 + k_4k_8 + k_2k_4)}$$

$$K_{1i} = \frac{k_6(k_2k_8 + k_3k_8 + k_4k_8 + k_2k_4)}{k_1k_6(k_3 + k_4)}$$

$$K_{2i} = \frac{k_1(k_3k_7 + k_4k_7 + k_5k_7 + k_3k_5)}{k_1k_6(k_3 + k_4)}$$

The Haldane relationship [35] for this model requires that

$$K_{eq} = \frac{V_1 K_2}{V_2 K_1} = \frac{k_1 k_3 k_5 k_7}{k_2 k_4 k_6 k_8} = 1.$$

Thus, with appropriate substitutions, Eqn 2 can be reduced to

$$v_{net} = \frac{V_1(S_1 - S_2)}{K_1(1 + S_2/K_2) + S_1(1 + S_2/K_{2i})} \tag{3}$$

C. Unidirectional transport. The rate of unidirectional transport is calculated from the initial rate of uptake for the radioactive substrate. The kinetic equations are derived using isotopic exchange methods [36]. In the following equations, the asterisk will denote labeled substrate or substrate-carrier complex. The rate of movement of label from side 1 to side 2 when $S_2^* = 0$ is given by Eqn 4.

$$v_{1\to 2}^* = k_3[ES_1^*] = \frac{k_1 k_3 k_5 S_1^*[E]}{(k_2 k_5 + k_2 k_4 + k_3 k_5)} \tag{4}$$

As was done for Eqn 2, [E] is derived by the method of King and Altman and substitutions for V_1, K_1, K_2 and K_{2i} are made according to the definitions given previously. However, one additional definition is required and that is:

$$R_2 = \frac{k_8(k_2 k_5 + k_2 k_4 + k_3 k_5)}{k_1 k_3 k_5}$$

Then, substitution into Eqn 4 yields:

$$v_{1\to 2}^* = \frac{V_1 S_1^*(1 + S_2/R_2)}{K_1(1 + S_2/K_2) + S_1(1 + S_2/K_{2i})} \tag{5}$$

The procedure we use to determine unidirectional transport measures the fraction of the labeled substrate in the blood that is extracted by the brain, $E = (S_1^*)_{1\to 2}/S_1^*$. Then, $v_{1\to 2}^* = ES_1^* F_p/W$ (see Methods). However, by multiplying both sides of Eqn 5 by S_1/S_1^*, it is possible to express unidirectional transport in terms of the unlabeled substrate concentration.

$$v_{1\to 2} = ES_1 F_p/W = \frac{V_1 S_1(1 + S_2/R_2)}{K_1(1 + S_2/K_2) + S_1(1 + S_2/K_{2i})} \tag{6}$$

This equation is equivalent to the one derived by Regen and Morgan [24] when the following substitutions are made for their constants F_s, K_{so}, K_{si}, R_s and B_s:

$$F_s = \frac{V_1}{K_1}; \quad K_{so} = K_1; \quad K_{si} = K_2; \quad R_s = R_2; \quad B_s = \frac{K_1 K_{2i}}{R_2}.$$

A major advantage of using Eqn 6 is that it facilitates the interpretation of data from double reciprocal plots. A plot of $1/v_{1\to 2}$ versus $1/S_1$ will have the following slope and intercept:

$$\text{Slope} = \frac{K_1(1+S_2/K_2)}{V_1(1+S_2/R_2)} \tag{7}$$

$$\text{Intercept} = \frac{(1+S_2/K_{2i})}{V_1(1+S_2/R_2)} \tag{8}$$

D. Kinetic constants for simplified models. The following simplifying assumptions have been evaluated in previous analyses of facilitated diffusion of glucose in the erythrocyte [4, 5, 11, 24–26, 37, 38]:

a. Translocation of the carrier-substrate complex is the rate-limiting step, i.e. $k_3, k_4, k_7, k_8 \ll k_1, k_2, k_5, k_6$.

b. The rate of translocation of free carrier is the same as that for substrate-carrier complex, i.e. $k_3 = k_4 = k_7 = k_8$.

Table I lists four separate models based on the two assumptions given above. When both assumptions are used, one obtains the simplest equation for unidirectional transport where $K_D = k_2/k_1$ (Eqn 9).

$$v_{1\to 2} = \frac{VS_1}{K_D+S_1} \tag{9}$$

This model is called symmetrical because $V_1 = V_2$ and the K, K_i and R values for both sides of the membrane are identical. In addition, the slope and intercept for a double reciprocal plot do not vary as a function of S_2 (Eqns 10 and 11).

$$\text{Slope} = K_D/V \tag{10}$$

$$\text{Intercept} = 1/V \tag{11}$$

The remaining 3 models listed in Table I are described by a kinetic equation identical to Eqn 6. Thus, when translocation is not the rate-limiting step or when the rates of translocation are unequal for loaded and unloaded carrier, both the slope and the intercept for a double reciprocal plot will be hyperbolic functions of S_2 (Eqns 7

TABLE I

ASSUMPTIONS USED IN VARIOUS MODIFICATIONS OF THE SIMPLE MOBILE-CARRIER MODEL OF FACILITATED DIFFUSION

Model	Translocation rate-limiting	Translocation rates equal	Kinetic equation
Symmetric	yes	yes	9
Semi-symmetric*	no	yes	6
Translocation-limited general**	yes	no	6
General	no	no	6

* This term was chosen because translocation rates as well as the dissociation constants for both sides of the membrane are equal; however, $V_1 \neq V_2$ and $K_1 \neq K_2 \neq R_2 \neq K_{2i}$.

** Although this model is a more restricted form of the general model, it is indistinguishable from the general model using our kinetic analysis.

and 8)*. Furthermore, if $R_2 > K_2$, the slope replot will be concave upwards (inhibition), while if $R_2 < K_2$ it will be concave downwards (activation). Similar results are obtained with the intercept replots since there is inhibition when $R_2 > K_{2i}$ and activation when $R_2 < K_{2i}$. Within any group of data where S_2 is constant, however, these models fit the Michaelis-Menten equation shown under Methods.

ACKNOWLEDGEMENTS

The authors gratefully acknowledge the technical assistance of Mr Paul Conway, Mr Wilbert Heiman, Mr Bruce Levin, Mr Alton Mitmoen, Mr Bill Patterson, Mr Mark Saffitz and Miss Karla Raab. This investigation was supported by Grants NS05961 and 6MO1932 from the National Institutes of Health and by University Surgical Associates. A. L. Betz is the recipient of a Medical Scientist Training Program award.

REFERENCES

1 Boos, W. (1974) Annu. Rev. Biochem. 43, 123–146
2 Stein, W. D. (1967) The Movement of Molecules across Cell Membranes, Academic Press, New York
3 Schultz, S. G. and Curran, P. F. (1970) Physiol. Rev. 50, 637–718
4 Kotyk, A. (1973) Biochim. Biophys. Acta 300, 183–210
5 Wyssbrod, H. R., Scott, W. N., Brodsky, W. A. and Schwartz, I. L. (1971) Handbook of Neurochemistry (Lajtha, A., ed.), Vol. 5, pp. 683–819, Plenum Press, New York
6 Buschiazzo, P. M., Terrell, E. B. and Regen, D. M. (1970) Am. J. Physiol. 219, 1505–1513
7 Betz, A. L., Gilboe, D. D. and Drewes, L. R. (1974) Brain Res. 67, 307–316
8 Heinz, E. and Durbin, R. P. (1957) J. Gen. Physiol. 41, 101–117
9 Heinz, E. and Walsh, P. M. (1958) J. Biol. Chem. 233, 1488–1493
10 Mawe, R. C. and Hempling, H. G. (1965) J. Cell Comp. Physiol. 66, 95–103
11 Levine, M., Oxender, D. L. and Stein, W. D. (1965) Biochim. Biophys. Acta 109, 151–163
12 Gilboe, D. D., Betz, A. L. and Langebartel, D. A. (1973) J. Appl. Physiol. 34, 534–537
13 Gilboe, D. D., Andrews, R. L. and Dardenne, G. (1970) Am. J. Physiol. 219, 767–773
14 Betz, A. L., Gilboe, D. D., Yudilevich, D. L. and Drewes, L. R. (1973) Am. J. Physiol. 225, 586–592
15 Fishman, R. A. (1964) Am. J. Physiol. 206, 836–844
16 Drewes, L. R. and Gilboe, D. D. (1973) J. Biol. Chem. 248, 2489–2496
17 Slein, M. W. (1965) Methods of Enzymatic Analysis (Bergmeyer, H. U., ed.), pp. 117–123, Academic Press, New York
18 Cleland, W. W. (1967) Adv. Enzymol. 29, 1–32
19 Betz, A. L., Gilboe, D. D. and Drewes, L. R. (1975) Am. J. Physiol. 228, 895–900
20 Crone, C. (1965) J. Physiol. Lond. 181, 103–113
21 Yudilevich, D. L., DeRose, N. and Sepulveda, F. V. (1972) Brain Res. 44, 569–578
22 Brightman, M. W., Klatzo, I., Olsson, Y. and Reese, T. S. (1970) J. Neurol. Sci 10, 215–239
23 Cremer, J. E. and Heath, D. F. (1974) Biochem. J. 142, 527–544
24 Regen, D. M. and Morgan, H. E. (1964) Biochim. Biophys. Acta 79, 151–166
25 Geck, P. (1971) Biochim. Biophys. Acta 241, 462–472
26 Regen, D. M. and Tarpley, H. L. (1974) Biochim. Biophys. Acta 339, 218–233
27 Lieb, W. R. and Stein, W. D. (1970) Biophys. J. 10, 585–609

* Although this relationship applies to the majority of models based on Fig. 6, a second unique situation occurs when it is assumed that $k_7 = k_8$ and translocation of the unloaded but not the loaded carrier is rate-limiting. In this case the slope is independent of S_2, while the intercept is a hyperbolic function of S_2.

28 Naftalin, R. J. (1970) Biochim. Biophys. Acta 211, 65–78
29 LeFevre, P. G. (1973) J. Membr. Biol. 11, 1–19
30 Drewes, L. R., Gilboe, D. D. and Betz, A. L. (1973) Arch. Neurol. 29, 385–390
31 Batt, E. R. and Schacter, D. (1973) J. Clin. Invest., 52, 1686–1697
32 Rosenberg, T. and Wilbrandt, W. (1963) J. Theor. Biol. 5, 288–305
33 Silverman, M. and Goresky, C. A. (1965) Biophys. J. 5, 487–509
34 King, E. L. and Altman, C. (1956) J. Phys. Chem. 60, 1375–1378
35 Cleland, W. W. (1963) Biochim. Biophys. Acta 67, 104–137
36 Cleland, W. W. (1967) Annu. Rev. Biochem. 36, 77–112
37 Lieb, W. R. and Stein, W. D. (1972) Biochim. Biophys. Acta 265, 187–207
38 Miller, D. M. (1968) Biophys. J. 8, 1339–1352